

할로이사이트 나노튜브를 포함하는 천연고무(NR)/Ethylene-Propylene-Diene Monomer(EPDM) 복합소재 연구

P. Ganeshan, M. S. Ravi Theja[†], P. Ramshankar*, and K. Raja**

Department of Mechanical Engineering, Sri Eshwar College of Engineering

*Department of Civil Engineering, College of Engineering Guindy, Anna University

**Department of Mechanical Engineering, University College of Engineering, Dindigul

(2022년 11월 30일 접수, 2023년 3월 14일 수정, 2023년 5월 22일 채택)

Halloysite Nanotubes (HNTs)-Reinforced Natural Rubber (NR)/Ethylene-Propylene-Diene Monomer (EPDM) Composites

P. Ganeshan, M. S. Ravi Theja[†], P. Ramshankar*, and K. Raja**

Department of Mechanical Engineering, Sri Eshwar College of Engineering, Coimbatore, Tamil Nadu - 64102, India

*Department of Civil Engineering, College of Engineering Guindy, Anna University, Chennai, Tamil Nadu - 600025, India

**Department of Mechanical Engineering, University College of Engineering, Dindigul, Dindigul, Tamil Nadu - 624622, India

(Received November 30, 2022; Revised March 14, 2023; Accepted May 22, 2023)

Abstract: Natural rubber/ethylene-propylene-diene monomer (NR/EPDM) rubber blends of composition 75/25 with 0, 2, 4, 6, 8, and 10 phr (parts per hundred rubber) halloysite nanotubes (HNTs) were prepared by two-roll mill. The effect of HNTs on the cure characteristics and mechanical properties of the NR/EPDM nanocomposites were studied. The effect of HNTs loading on the morphological, physical, swelling resistance and compression set of nanocomposites based on NR/EPDM was also investigated. Tensile strength tests revealed that the HNTs-reinforced NR/EPDM composite could resist 84% greater strength to break than the NR/EPDM blend without reinforcement. The introduction of HNTs into the NR/EPDM rubber matrix induced a rough morphology in the fracture surface, and a well-dispersed structure was obtained with the inclusion of up to 8 phr of HNTs, according to the morphological analyses.

Keywords: natural rubber/ethylene-propylene-diene monomer, halloysite nanotubes, mechanical properties, swelling resistance, morphology.

Introduction

Blending two rubbers is an effective way to increase qualities that aren't inherent in a single rubber. The adhesion between the components determines the qualities of any blend. Despite the fact that the majority of the mixes are thermodynamically incompatible, many have been discovered to be technologically important.¹⁻³ When natural rubber (NR) is stretched, it can crystallise. Stress-induced crystallisation can be utilised to increase modulus and deformation resistance, preventing defects from propagating. Ethylene-propylene-diene monomer (EPDM) rubber, on the other hand, comprises saturated hydrocarbon backbones, which provide excellent weathering, oxidation,

and chemical resistance.^{4,5} Compounds with good ozone and chemical resistance and reduced compression set have been created by combining NR with EPDM and other diene rubbers. NR is frequently added to EPDM to increase the tack qualities of the material.⁶ Because EPDM chains have different unsaturated bonds than NR chains, this combination may have poor curing qualities. These two rubbers, NR and EPDM, are non-polar and incompatible.⁷ Each of them possesses certain advantageous physical and chemical characteristics that, when combined, would provide useful commercial products. As a result, ethylene propylene diene monomer-*grafted*-maleic anhydride (EPDM-g-MA) is utilised as a compatibilizer to compensate for this weak point.⁸⁻¹⁰ The mechanical properties of the blend will also be greatly impacted by the phases' adhesion. The compatibilizer is utilised because it plays a crucial part in achieving the required properties of the compositions through

[†]To whom correspondence should be addressed.
thejaneeds@gmail.com, ORCID[®] 0000-0002-9450-5530
©2023 The Polymer Society of Korea. All rights reserved.

the process that blends these incompatible polymers.¹¹⁻¹³ The interfacial adhesion was increased by a number of experiments. Some of these included modifying the EPDM so that the mix would be compatible with it after being exposed to reactive chemicals like maleic anhydride during the peroxide initiation process, halogenating the EPDM in solution, and using accelerators that were more soluble in the EPDM phase.¹⁴⁻¹⁶ Unfortunately, there are very few research examining immiscible polymer mixes with solid particle-stabilized surfaces. Immiscible polymer blends can now be made compatible economically by adding inorganic nanoparticles. It has been demonstrated that the nanoparticles may significantly absorb at the blend's interface, which enables them to stabilise it.¹⁷⁻¹⁸

Fillers are being incorporated into polymeric materials to improve their qualities for end-use applications, according to researchers.¹⁹⁻²⁰ In most cases, nanometer-sized inorganic fillers are used as reinforcing elements in polymers. Because of its high surface area, high aspect ratio (*i.e.*, length/thickness or length/diameter ratio), low density, and presence of functional groups on the surface, the reinforcing effect can be achieved at lower filler concentrations than micron-sized fillers. Because the strength and modulus of gum rubber are relatively low, elastomers are reinforced with hard and soft materials to achieve practical use of rubber products.²¹⁻²² Carbon black, silica, and fibres are common fillers in the rubber industry.²³ Traditional fillers, on the other hand, are needed in high quantities (30-60%) to provide the best qualities for the final applications. As a result, nano-sized inorganic particles have gotten a lot of attention in the rubber sector.²⁴⁻²⁵ Organic/inorganic hybrid nanocomposites are often made from naturally occurring clays and minerals having at least one dimension in the nanometer range (1-100 nm). Nanoclays are commonly employed in elastomers because they may fine-tune their surface chemistry by adding functional groups.²⁶⁻²⁷ Nanosized graphene and carbon nanotubes (both functionalized and nonfunctionalized) reinforced rubber are a promising new class of advanced materials in the rubber sector for increasing electrical conductivity as well as mechanical qualities.²⁸⁻³⁰

Halloysite nanotubes (HNTs) are aluminosilicates having a hollow micro and nanotubular structure comparable to carbon nanotubes that occur naturally. Its high mechanical strength and Young's modulus (≈ 1 TPa) make it a unique and adaptable material for polymer nanocomposites preparation. The hydrated form (with interlayer spacing of 10 Å) of layered halloysite with the formula $\text{Al}_2\text{Si}_2\text{O}_5(\text{OH})_4 \cdot 2\text{H}_2\text{O}$ and the anhydrous form (with interlayer spacing of 7 Å) of layered halloysite with the

formula $\text{Al}_2\text{Si}_2\text{O}_5(\text{OH})_4$ are the two forms of layered halloysite nanotubes. Because of its unusual structure and the presence of functional groups on its surface, it can be used in both biological and nonbiological applications. Anticorrosion agents, thermal resistance, cargo for biomaterials, prospective drug delivery vehicle, immobilisation matrix, and polymerization processes are only a few of the applications of HNTs in the polymeric sector.³¹⁻³⁴ Several attempts have been made recently to use various kinds of nanoscale reinforcements to create a rubber compound based on NR/EPDM mixes that has the requisite mechanical qualities. The impact of organoclay on the shape and mechanical characteristics of NR/EPDM blends with varying content ratios was described by Alipour *et al.*³⁵ They discovered a 40% rise in tensile modulus when 7 phr of organoclay is added to the NR/EPDM (75/25 phr/phr). The aim of the present work is to study the cure characteristics, mechanical, abrasion resistance and morphology of NR/EPDM/EPDM-g-MA blends reinforced with HNTs with special reference to the effects of HNTs content. The behaviour of the composites in different solvent was also examined.

Experimental

Materials. All mixing ingredients were used as received.

Rubber materials: Natural rubber (NR: Ribbed Smoked Sheets (RSS)-1, $\text{ML}_{(1+4)}$ 100 °C - 57 M, density - 0.9125 g/cm³, ash content - 0.58% and nitrogen content - 0.63%) and ethylene-propylene-diene monomer (EPDM) rubber (KEP-270, $\text{ML}_{(1+4)}$ 125 °C - 60 M, ethylene content - 68 wt%, termonomer content (ethylidene norbornene) - 4.5% and density - 0.86 g/cm³) were procured by Asian Rubber Pvt. Ltd., Ambattur, Chennai, India and Supple Rubber Chemicals Pvt. Ltd., New Delhi, India, respectively.

Reinforcement: Halloysite nanotubes (family: kaolin clay), linear chemical formula: $\text{Al}_2\text{Si}_2\text{O}_5(\text{OH})_4 \cdot 2\text{H}_2\text{O}$, molecular weight: 294.19 g/mol, diameter \times length: 30-70 nm \times 1-3 μm was obtained from Sigma-Aldrich, Puducherry.

Rubber Chemicals: Activator (stearic acid and zinc oxide), accelerators (mercaptobenzothiazyl disulphide - MBTS, tetramethylthiuram disulphide - TMTD), zinc diethyldithiocarbamate (ZDC) and 2-mercaptobenzothiazole - MBT) and vulcanizing agent (sulphur) were obtained from Vignesh Chemicals Pvt. Ltd., Ambattur, Chennai, India.

Compatibilizer: Ethylene-propylene-diene rubber *grafted* with maleic anhydride (EPDM-g-MA), with the trademark Bondyram[®] 7001, was purchased from Songhan Plastic Technology Co.

Table 1. Formulation of NR/EPDM-HNTs Compounds

Sample code	Compounds (phr)								
	NR	EPDM	EPDM-g-MA	HNTs	Zinc oxide	Stearic acid	MBTS	TMTD	Sulphur
H_0	75	25	5	0	4	1.5	1.2	1	2.5
H_2	75	25	5	2	4	1.5	1.2	1	2.5
H_4	75	25	5	4	4	1.5	1.2	1	2.5
H_6	75	25	5	6	4	1.5	1.2	1	2.5
H_8	75	25	5	8	4	1.5	1.2	1	2.5
H_{10}	75	25	5	10	4	1.5	1.2	1	2.5

Ltd., Shanghai City, China with melt flow rate (MFR) of 7 g/10 min (ASTM D D1238), mass density of 0.87 g/cm³ (ASTM D792) and MAH content of 0.7%.

Swelling Chemicals: Aromatic solvents (benzene, mesitylene, toluene and xylene), aliphatic solvents (*n*-pentane, *n*-heptane, *n*-hexane and *n*-octane) and chlorinated solvents (chloroform, dichloromethane and carbon tetrachloride) employed in this study were supplied by Sigma-Aldrich, Puducherry.

Preparation of Nanocomposites. An open-mill mixer was used to produce the NR/EPDM mixes with varying filler loadings. Mastication and blending of each polymer were done individually between mill rolls at room temperature, according to the formulas in Table 1. The NR rubber was masticated for around 5 minutes in a two-roll mill, then EPDM-g-MA and EPDM were added for another 5 min on the same mill, followed by the vulcanization components. HNTs were added five minutes after the components were added, and the nanocomposite was stirred for five to fifteen minutes. Depending on the filler loading, the compounding time for each composite was kept at 20-30 min. The composites were vulcanised in a hydraulic press (platen size: 15×15 cm) at a pressure of 60 MPa, at a temperature of 160 °C, and for an optimum cure period.

Characterization. Cure characteristics: The cure properties of the unvulcanized rubber samples were assessed using an oscillating disc rheometer at 160 °C in accordance with ASTM D2084 (ODR).

Tensile strength, elongation at break and 100% modulus: A die cutter was used to cut dumbbell-shaped and un-nicked 90-degree test shaped samples from the moulded sheets. The composites were tensile tested in accordance with ASTM D412-C using a universal testing machine (UTM) (series: 7200, make: Dak System Inc., model: T-72102) at 23 °C and 500 mm/min cross-head speed.³⁶ Using the aforementioned equipment and testing circumstances, tear characteristics were determined according to ASTM D624-B. For each series of studies, at least

five samples were evaluated to provide a high level of confidence.

Hardness and abrasion resistance: The shore A durometer hardness tester was used to assess hardness in accordance with ASTM D2240. Based on ASTM D5963, an abrasion resistance test (Zwick abrasion tester) was performed. A vertical rebound resilience tester was used to measure rebound resilience in accordance with ASTM D2632.³⁷⁻³⁸

Crosslink Density: The crosslink density of rubber specimens was measured on the basis of the immersion techniques (equilibrium solvent-rubber swelling) measurements (toluene uptake for 72 h at 23 °C) by applying the Flory–Rehner equation.³⁹⁻⁴²

$$M_c \left(\frac{\text{g}}{\text{mol}} \right) = \frac{-\rho_p V_s V_r^{1/2}}{\ln(1 - V_r) + V_r + \chi V_r^2} \quad (1)$$

where, M_c is the molar mass of the polymer between crosslinks, V_s is the molar volume of the solvent (106.3 mL/gmol), ρ_p is the density of the polymer, V_r is the volume fraction of polymer in the solvent-swollen filled compound, χ is the interaction parameter of the polymer (0.25),⁴³ and V_r is given by following eq.⁴⁴

$$V_r = \frac{1}{1 + Q_m} \quad (2)$$

where, Q_m is the weight swell of the NR/EPDM-HNTs nanocomposites in toluene.

The degree of crosslink density (ν) is given by eq. (3):

$$\nu \left(\frac{\text{mol}}{\text{cm}^3} \right) = \frac{1}{2M_c} \quad (3)$$

Swelling Resistance Property: The equilibrium immersion swelling method was used to assess swelling resistance, which is expressed as mole percent uptake in a swollen state. Rubber samples were swollen in different chemicals/solvents (benzene, mesitylene, toluene, xylene, *n*-pentane, *n*-heptane, *n*-

hexane, *n*-octane, chloroform, dichloromethane and carbon tetrachloride) at ambient temperature (23 °C) for 3 days and then removed from the solvent and the rubber surface solvent was blotted off rapidly with help of tissue paper. The rubber samples were immediately weighed on an analytical balance. The mole percent uptake Q_t was determined using the formula.

$$Q_t(\text{mol}\%) = \frac{(M_t - M_0)/MW}{M_0} \times 100 \quad (4)$$

where, M_t is the mass of the specimen after 3 days of immersion, M_0 is the initial mass of the specimen and MW is the molecular weight of the solvent.

Compression Set: Using an assembled apparatus, the test was conducted at both ambient and high temperatures. According to ASTM D395, a compression set test was performed. The compressive stress was calculated at 25% of the original thickness. The constructed device was aged in a dry-air circulating oven for 22 hours at 70 °C for elevated temperature testing. The recovery % of rubber material in terms of compress thickness is referred to as compression set. It is calculated using eq. (5).

$$\text{Percentage of compression set, } C\% = \frac{A_0 - A_1}{A_0 - A_s} \times 100 \quad (5)$$

where, A_0 is the original thickness of the specimen, A_1 is the specimen thickness after removed from the compression device and A_s is the spacer bar thickness which is used.

SEM Microscopy: A field emission-scanning electron microscope (FE-SEM) type Hitachi S-3400 operating at a voltage of 30 kV was used to examine the tensile fracture surface. The goal was to get a concept of the mechanism of fracture. To avoid electrical charge during examination, the fracture ends of the tensile specimens were mounted on stubs and sputter coated with a thin layer of gold.

Results and Discussions

Figures 1(a-f) show the curing behaviours of NR/EPDM-HNTs nanocomposites containing various concentrations of HNTs. The presence of HNTs and its loading on the curing behaviours of the NR/EPDM-HNTs nanocomposites can be investigated using these figures. The maximum torque (M_h) of the NR/EPDM-HNTs nanocomposites progressively increases as the concentration of HNTs in the nanocomposites increases, as shown in Figure 1(a). A M_h represents the stiffness or shear modulus of test specimens that have undergone complete vul-

canization at the curing temperature. The inclusion of HNTs, which has a stronger limitation on the molecular motion of the macro molecule or tends to impose additional flow resistance, was the cause of the enhancement M_h of the HNTs filled nanocomposites.⁴⁵ This reflects the material's rigid filler HNT's reinforcing action, which increases the modulus and hardness of the NR/EPDM-HNTs nanocomposite.

The minimum torque (M_i) is another significant factor that affects the rubber compound's viscosity. Figure 1(b) shows the M_i of NR/EPDM-HNTs composites. The reinforcing effect of HNTs nanofiller and its interaction with the macromolecular chains of the polymer matrix could explain the increase in viscosity of the rubber compounds with varying HNTs content seen in Figure 1(b). This is most likely owing to the EPDM-g-MA compatibilizer and other additives present. The flow ability of the NR/EPDM-HNTs composites decreases as the HNTs concentration increases, resulting in an increase in M_i . The interfacial interaction between the nanotubes and the rubber matrix chains is improved due to the presence of HNTs with a high aspect ratio in the rubber composite. When more HNTs are introduced to the NR/EPDM matrices, the effect becomes more dramatic. The mobility of NR/EPDM rubber chains is limited by physical interactions between scattered HNTs and rubber matrix molecular chains. Therefore, the resistance of the rubber compound against flow (M_i) progressively increases with HNTs content.

Figure 1(c) depicts the delta torque of several samples. As the concentration of HNTs in the rubber vulcanizate is raised, the delta torque (ΔM), which is a measure of crosslink density of the rubber nanocomposite, also increases. The higher ΔM in the NR/EPDM nanocomposite with HNTs implies an increase in compound crosslink density with HNTs loading. These findings show that HNTs have a strengthening impact in the NR/EPDM nanocomposite while also causing a more efficient curing process in the rubber compound. The existence of positive and negative ions on the inner and outer surfaces of HNTs scattered in the rubber matrix contributes to the latter function of HNTs in the rubber composite. Similar findings have been made regarding ΔM , which measures the difference in shear modulus or stiffness between test specimens that have been fully vulcanised and those that have not, as measured at the lower end of the vulcanizing curve. The cross-link density is indirectly correlated with the ΔM .⁴⁶ Consequently, it may be said that the addition of HNTs has improved cross-linking.⁴⁷

The scorch time (t_{s2}), optimum cure time (t_{90}), and cure rate index (CRI) of NR/EPDM-HNTs nanocomposites are shown

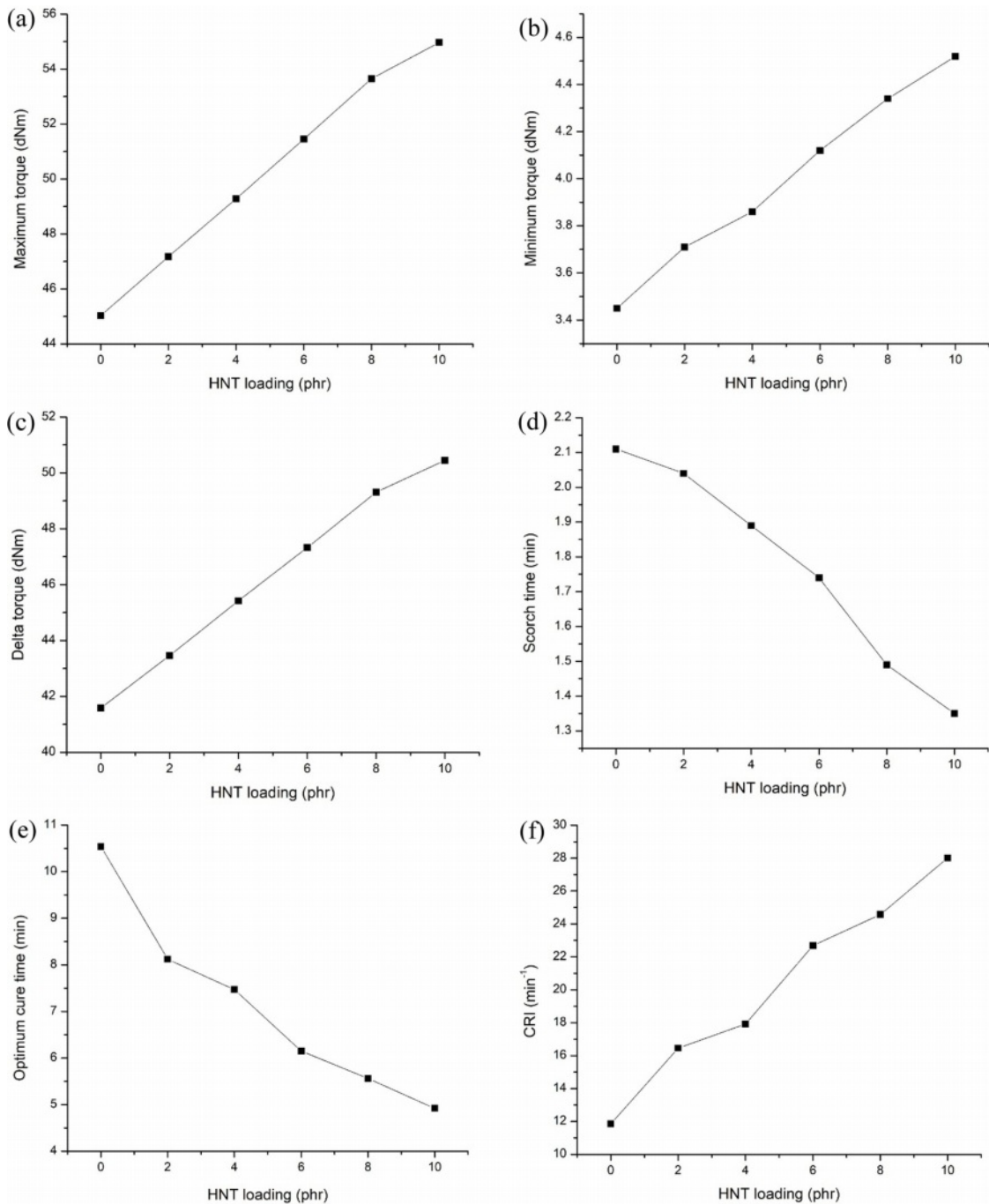


Figure 1. Cure behaviors of NR/EPDM-HNTs composites: (a) M_n ; (b) M_i ; (c) ΔM ; (d) t_{s2} ; (e) t_{90} ; (f) CRI

in Figures 1(d)-(f) respectively. Scorch time is an important parameter of cure behavior that influences the processing of rubber composites. As the amount of HNTs in the NR/EPDM-HNTs composites increase, the t_{s2} and t_{90} of the composites dropped. The existence of positive and negative ions on the surfaces of HNTs, as well as their large surface area, could explain the variation in t_{s2} . Figure 1(d) shows that the inclusion

of HNTs reduced the t_{s2} of the NR/EPDM-HNTs composites, with the t_{s2} steadily decreasing as the amount of HNTs in the nanocomposites increased. The results show that including HNTs into the NR/EPDM matrices decreased the t_{90} of the nanocomposites. HNTs have been used in polymer composites not only as reinforcement agents to improve mechanical characteristics, but also as curing accelerators. The presence of

HNTs in rubber compounds results in a greater cure rate and earlier crosslinking activation, according to these figures. Adding HNTs to rubber composites with a constant amount of EPDM-g-MA compatibilizer, on the other hand, has resulted in an increase in overall curing qualities.

Figures 2(a-c) show the change in mechanical characteristics of NR/EPDM-HNTs nanocomposites as a result of tensile testing. As shown in Figure 2(a), increasing the content of HNTs in the NR/EPDM-HNTs nanocomposites gradually raises the tensile strength of the nanocomposites up to 8 phr before decreasing. Because of interactions between the rubber blend and HNTs, a higher crosslinking density, and the stiffening effect of HNTs, the introduction of HNTs resulted in a higher tensile strength.⁴⁸ Figure 2(a) further shows that adding the optimum loading of HNTs, which was around 8 phr, increased the tensile strength of the rubber blend matrix by up to 84%. The dependence of tensile strength augmentation with HNT concentration declines above 8 phr loading, and nano-reinforcement effectiveness becomes negligible. Tensile strength increased at a relatively fast rate at beginning (below 8 phr of HNT), but when HNT concentration increased (above 8 phr of HNT), this rate diminished, resulting in a downward trend in tensile strength. The creation of HNT agglomerations, which caused filler–filler interaction growth (confirmed by FE-SEM observation displayed in Figure 11), appears to have harmed the tensile strength enhancement. The findings revealed that until HNTs are finely disseminated into the polymer matrix in random orientation, the maximum improvement in tensile strength may be reached with their incorporation. Because of the decreased interfacial interaction induced by improper dispersion of HNTs, agglomeration of HNTs at higher loading reduces the enhancing impact of HNTs.

The influence of HNTs on the elongation at break of NR/EPDM-HNTs nanocomposites is shown in Figure 2(b). The elongation at break of NR/EPDM-HNTs rubber nanocomposites rises up to 8 phr with increasing HNT concentration before decreasing. The incorporation of HNTs into the NR/EPDM rubber matrix improves nanocomposites' elongation at break. Both tensile strength and elongation at break increased when the matrix/HNTs interactions were favourable and the HNTs content was low. The elongation at break of the NR/EPDM-HNT nanocomposites was significantly reduced as the concentration of HNTs in the formulation increased, which can be attributed to the stiff HNTs' restrictions in chain mobility and flexibility of the rubber matrix.⁴⁹⁻⁵⁰ The nanocomposites made of NR and EPDM have significantly increased flexibility and tensile strength.

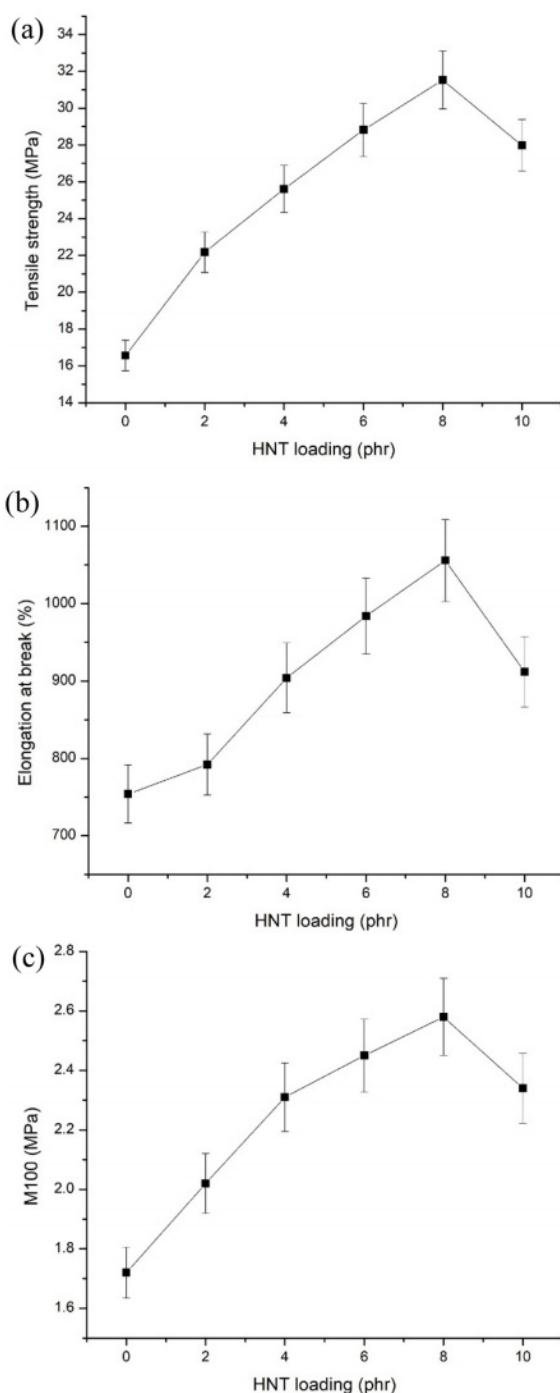


Figure 2. Mechanical characteristics of NR/EPDM-HNTs composites: (a) Tensile strength; (b) elongation at break; (c) M100

A physical barrier against a break is thought to be formed by the homogeneous distribution of HNTs throughout the rubber matrix, increasing the resistance to breaking. These findings suggest that the intercalation of rubber molecules into the galleries of HNT, even if each tube of the HNTs is not entirely

delaminated, can effectively improve the strength and toughness as well as the stiffness of NR/EPDM nanocomposites.

Figure 2(c) shows the variance in stress at 100% elongation (100% modulus, M100) for NR/EPDM-HNTs nanocomposites as a function of HNT concentration. These findings revealed that the change in stress at 100% elongation with HNT loading followed the same pattern as the tensile strength trend. M100 in nanocomposites increased up to 8 phr as the HNT content in the composites increased, then declined. This characteristic increased with HNT content, peaked at 6-8 phr, and then began to decline. The uniform distribution of HNTs in the rubber matrix, as evidenced by FE-SEM morphological investigations, the rigidity of the HNTs, and the interaction between rubber matrix and HNTs all contributed to the rise in M100 of NR/EPDM-HNTs composites, even at low HNT concentrations.⁵¹⁻⁵² Because of the formation of aggregates, nanofiller dispersion in rubber matrix is low at 10 phr. As a result, the interaction between the HNTs nanofiller and the NR/EPDM rubber matrix was reduced, and the M100 was reduced.

Figure 3 shows a plot of tear strength of NR/EPDM-HNT composites. The tear strength of the NR/EPDM nanocomposites increased when the amount of HNT in the compound was increased. The tear strength of the composite reinforced with 10 phr HNT was 53.41 N/mm, compared to 38.96 N/mm for the control sample (H_0). In most rubber matrixes, the tear process is divided into two stages: fracture initiation in crack-free regions and crack propagation to the failure point. For determining the influence of nanomaterials on rubber tear, both methodologies, including fracture initiation and crack propagation, should be examined. Several tear strength characteristics (induced stiffness, restricted rubber chain mobility, etc.) that

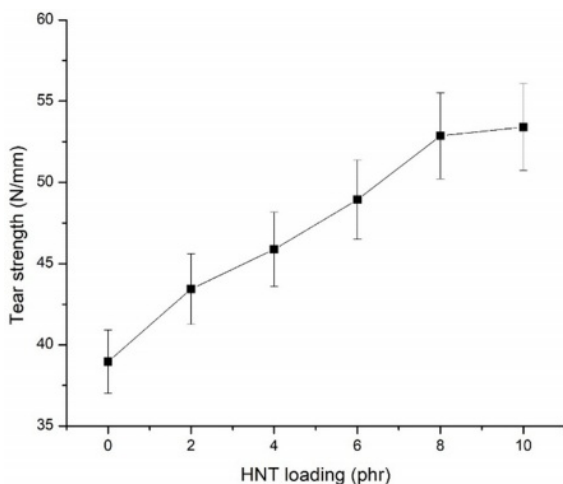


Figure 3. Tear strength of NR/EPDM-HNTs composites.

contribute to the increased tear strength of elastomers filled with nanofillers should also be considered. Furthermore, some nanofillers can act as reactive fillers by increasing the cross-link density of the rubber matrix and establishing a suitable filler–matrix interaction. The inclusion of nanofillers has also been linked to a reduction in crack propagation rate. The observed trend for tear strength, on the other hand, revealed that tear strength variables such as fine uniform dispersion of HNTs, high cross-link density, better HNT–rubber phase interaction, and low crack propagation rate are prominent, enhancing tear strength. It is clear that the HNTs loaded NR/EPDM nanocomposites' H_2 , H_4 , H_6 , H_8 , and H_{10} had tear strengths that were, respectively, 11, 18, 26, 36, and 37% higher than those of their corresponding control H_0 . Similar results are obtained in 8- and 10-phr filler-filled nanocomposites.

Figure 4 depicts the effect of HNTs loading on the hardness of the NR/EPDM nanocomposites. Hardness values rise monotonically with HNT content, as may be shown. These findings revealed that the change in hardness value with HNT loading followed the same pattern as the tear strength trend. The hardness of nanocomposites was substantially dependent on the HNT loading at low HNT concentrations, but this dependency gradually diminished as the HNT concentration increased. The intrinsic stiffness of HNTs, higher cross-link density, and the physical interaction between HNTs and rubber all contributed to the rise in hardness with increasing HNT content. These can limit the segmental motions of rubber chains, lowering the energy dissipation capabilities of nanocomposites and, as a result, preventing needle penetration, which is used to determine the degree of hardness.

As illustrated in Figure 5, the NR/EPDM-HNTs composite's

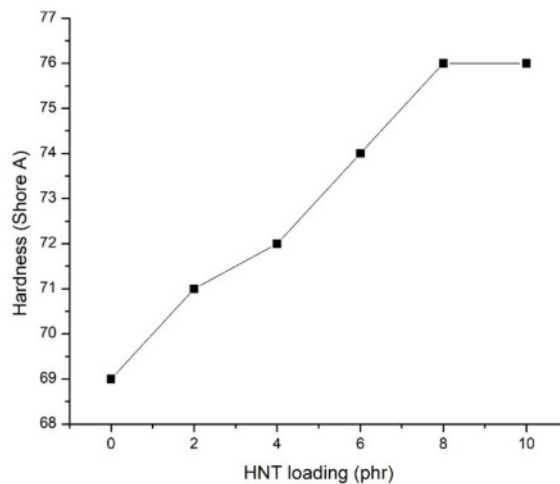


Figure 4. Hardness of NR/EPDM-HNTs composites.

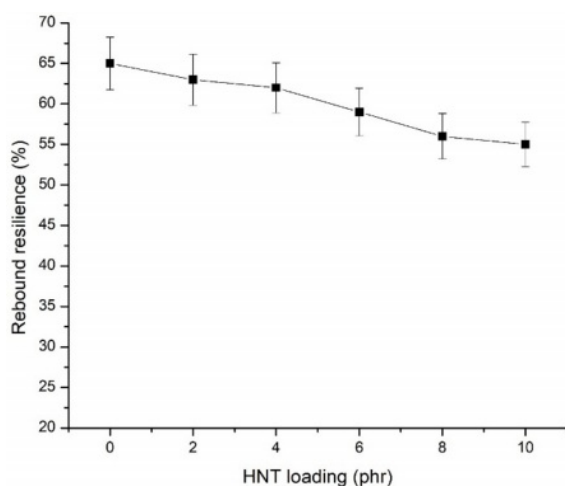


Figure 5. Rebound resilience of NR/EPDM-HNTs composites.

rebound resilience decreases as the concentration of HNTs nanofiller increases. According to ASTM D945, resilience is defined as the ratio of energy expended on deformation recovery to the energy necessary to cause the distortion. The flexibility of molecular chains is related to resilience; the more flexible the molecular chains are, the stronger the resilience.

Figure 6 shows the abrasion resistance of NR/EPDM-HNTs nanocomposite samples as a measure of the solid material's ability to withstand the progressive volume reduction from its surface by mechanical action. The abrasion resistance of the NR/EPDM nanocomposite samples was found to drop somewhat as the HNTs content was increased, going from 37.29 mm³ for the control NR/EPDM mix to 26.21 mm³ for the composite containing 10 phr of HNTs. This suggested that the NR/EPDM rubber matrix with higher reinforcement had better abrasion resistance against wear, which is an indirect indication of more cross-links and good interactions between the rubber matrix and HNTs. HNTs supported a portion of the applied load during the abrasion test, resulting in a reduction in penetration into the polymer surface and only allowing micro-plowing and/or micro-cutting processes to occur.⁵³

Figure 7 shows the estimated M_c and crosslink density values for NR/EPDM-HNTs composites. M_c values in HNTs-filled systems are lower than in unfilled rubber matrix, indicating a smaller molar mass between crosslinks, and M_c decreases as HNTs content increases. The accessible volume between adjacent cross-links reduced as the value of M_c decreased. The solvent uptake mechanism is hampered by the reduction in volume. As demonstrated in the FE-SEM micrographs, the modest rise in M_c at HNTs concentration more than 8 phr is attributable to the nanofiller aggregation. The estimated crosslink density

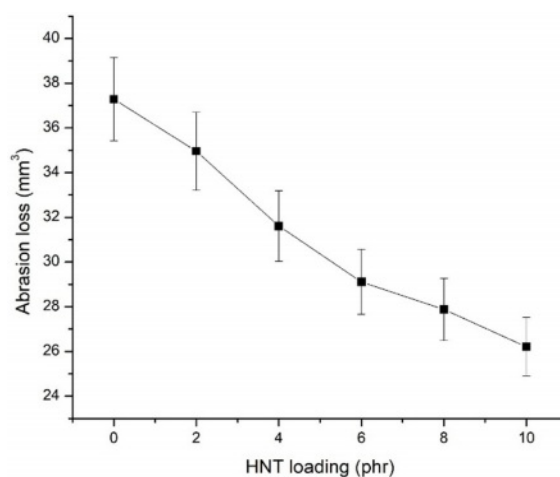


Figure 6. Abrasion loss of NR/EPDM-HNTs composites.

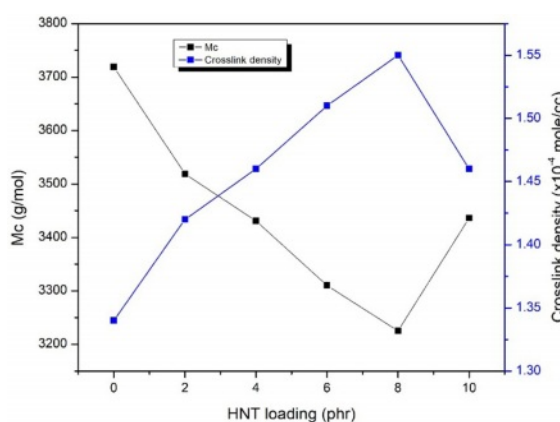


Figure 7. M_c and crosslink density of NR/EPDM-HNTs composites.

graphs supported this claim. The crosslink density increased as the nanofiller concentration in the composites increased, with a peak value of 8 phr. There was a decrease in crosslink density when the HNTs content was greater than 8 phr.

Rubber and other materials must maintain their dimensional stability when used in real-world conditions, which frequently involve purposeful or unintentional interaction with solvents and chemicals. The influence of HNTs loading on the swelling behaviour of the NR/EPDM-HNTs rubber nanocomposites in terms of mole percent uptake (Q_t) was explored in this study, and the findings are shown in Figure 8. The mole percent uptake of four aromatic (mesitylene, xylene, toluene, and benzene), four aliphatic (*n*-octane, *n*-heptane, *n*-hexane, and *n*-pentane) and three chlorinated solvents (carbon tetrachloride, chloroform, and dichloromethane) through NR/EPDM-HNTs nanocomposites in the temperature of 23 °C (ambient) were examined in the present work, with special reference to the effects of the HNTs loading and solvent size.

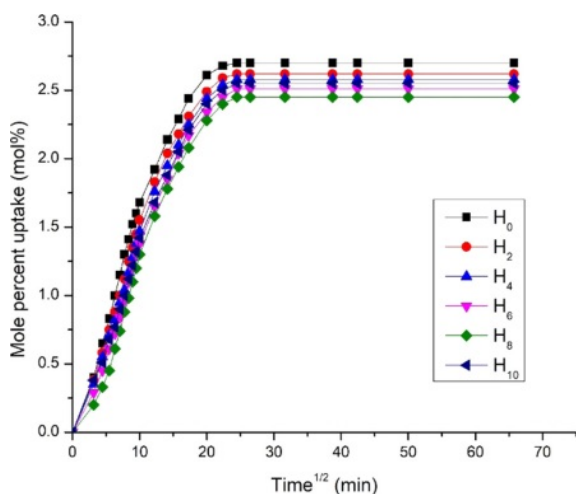


Figure 8. Mole percent uptake of mesitylene by different nanotubes loading.

The effect of HNTs content on mesitylene uptake is seen in Figure 8. It was discovered that gradually increasing the amount of HNTs resulted in a decreased mole percent uptake. The addition of 8 phr of HNTs into the NR/EPDM rubber matrix caused a notable reduction in the solvent uptake of the NR/EPDM-HNTs nanocomposites. The decrease in solvent uptake suggests that HNTs dilute and constrain the rubber matrix, limiting the extensibility of rubber chains generated by swelling.⁵⁴ Furthermore, the scattered structure of HNTs in rubber matrix, as well as interfacial interactions between the aluminols and silanols of HNTs with the matrix, limited solvent penetration.⁵⁵ The solvent uptake increased marginally after 8 phr. The creation of HNT agglomerates, as seen in the FE-SEM micrographs, was the reason for this. Different solvents (xylene, toluene, benzene, *n*-octane, *n*-heptane, *n*-hexane, *n*-pentane, carbon tetrachloride, chloroform, and dichloromethane) showed similar trends in mole percent uptake.

The influence of penetrant size on the mole percent uptake of four aromatic solvents through sulphur cured NR/EPDM-HNTs composites is shown in Figure 9(a). The graph shows that the trend is in the following order: benzene > toluene > xylene > mesitylene. The effect of penetrant size on the mole percent uptake of four aliphatic solvents via the same nanocomposites is shown in Figure 9(b). The graph shows that the tendency is in the following order: *n*-pentane > *n*-hexane > *n*-heptane > *n*-octane. The effect of penetrant size on the mole percent uptake of four chlorinated solvents through NR/EPDM rubber-HNTs nanocomposites is shown in Figure 9(c). The graph shows that the tendency is dichloromethane > carbon tetrachloride > chloroform in that order. With the exception of

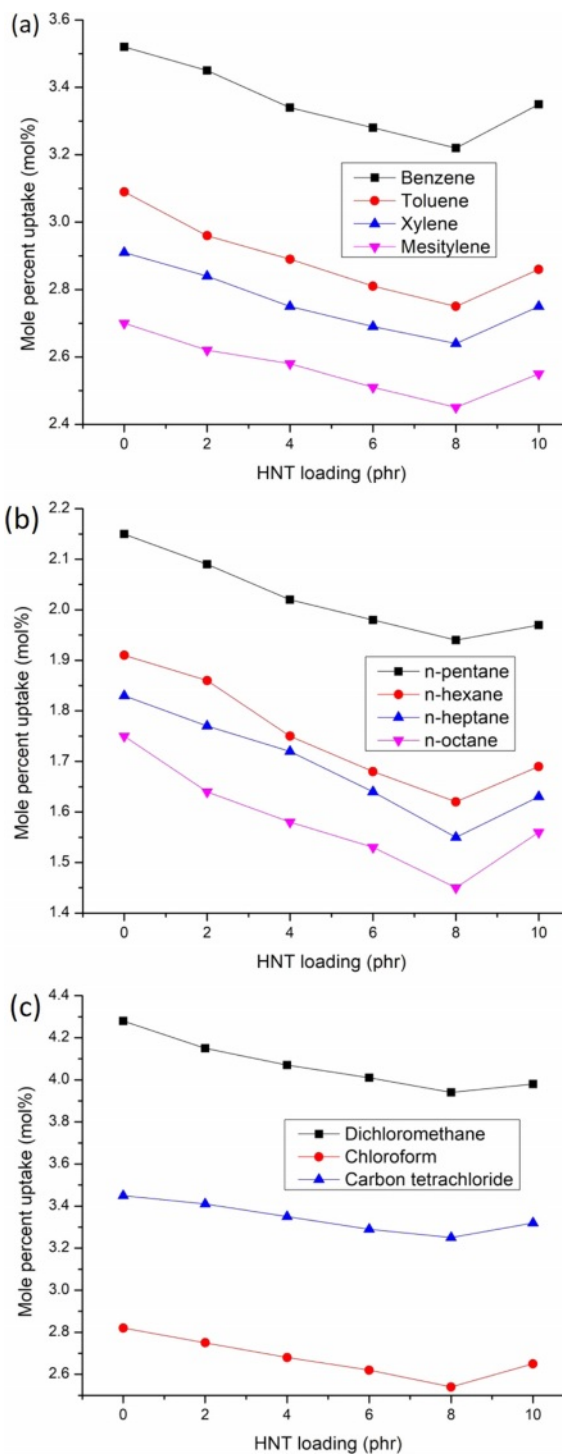


Figure 9. Mole percent uptake of different solvents through HNT filled NR/EPDM nanocomposites: (a) aromatic solvents; (b) aliphatic solvents; (c) chlorinated solvents.

chloroform, which displays a lower mole percent uptake increase at equilibrium (Q_e) levels than expected, the observations are in the correct order of the typical influence of the solvent's molecular

mass on mole percent uptake. Dichloromethane has the maximum uptake due to the solubility parameter's supremacy over the solvent's molecular mass during penetration. The smaller the discrepancy, the superior is the similarity of a polymer compounds toward the solvent.

More chemical crosslinks between elastomer chains in the vulcanizate with greater HNT loading, as found in curing tests (Figure 1(c): delta torque), may contribute to the observed reduction in mole percent uptake by preventing rubber molecules from being surrounded by solvent molecules.⁵⁶ As a result, a higher number of crosslinks turns the rubber matrix into a stiffer material that is less susceptible to solvent penetration. The increased amount of crosslinking causes a steady decrease in mass swell as HNTs loading increases. The geometry of the filler (size, shape, size distribution, concentration, and orientation), the characteristics of the filler, the properties of the rubber matrix, and the interaction between the rubber matrix and the filler all influence the mole percent uptake of solvent via a composite.⁵⁷ The nanocomposites' mole percent absorption is significantly lower than that of the unfilled NR/EPDM rubber matrix. The concentration of free space available in the polymer matrix to accommodate the penetrant molecule determines the penetrant solvent's uptake.⁵⁸ The incorporation of HNT limited the availability of these free spaces, limiting the rubber matrix's segmental mobility and creating a tortuous path for solvent molecules to transport through the nanocomposites.

Compression set is the ratio of elastic to viscous components of a rubber response to a particular deformation, and it assesses the ability of cured rubber to restore its original shape after the deforming force is withdrawn.⁵⁹⁻⁶⁰ The compound with the lowest compression set has the best elasticity and, as a result, the lowest viscosity. The ability of samples to keep their elasticity under stress is determined by the compression set. Figure 10 shows that the compression set values for filled systems are greater, indicating a loss in elasticity due to the better interaction between the rubber matrix and the filler. Due to the filler–filler network formation, compression set increases as a function of filler loading, reaching a maximum at 8 phr of HNTs content and decreasing at higher loading. The lower the compression set %, in general, the better. Compression set is a crucial characteristic of industrial rubber products notably sealants.

To investigate the effect of HNTs on the fracture surface morphology of NR/EPDM-HNTs nanocomposites, and FE-SEM micrographs of the elastomer blend control sample encoded as H_0 , composites with 8 phr of HNTs sample encoded as H_8 , and

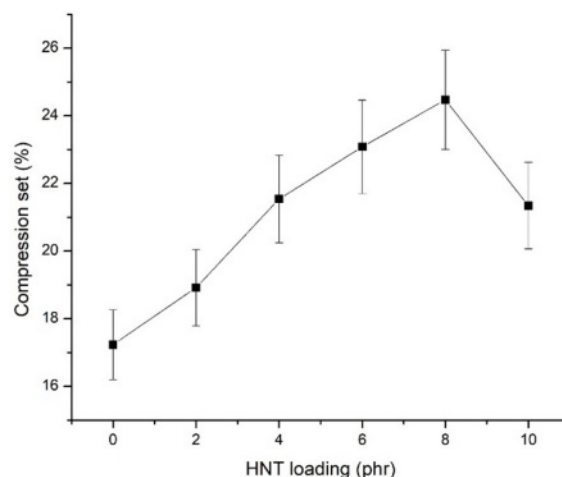


Figure 10. Compression set of NR/EPDM-HNTs composites.

composites with 10 phr of HNTs sample encoded as H_{10} are illustrated in Figure 11(a-c). The rough fracture surface of H_8 (Figure 11(b)) in comparison with H_0 (Figure 11(a)) was illustrative of good interactions between rubber matrix and HNTs, likely attributed to the penetration of the elastomer chains into the cluster of HNTs with no observable agglomeration.

FE-SEM micrographs confirmed the good dispersion of HNTs throughout the polymer matrix, where HNTs appeared as white cylindrical particles in FE-SEM micrographs. It seems that HNTs were predominately located in the NR phase which appears darker gray than the EPDM phase owing to its higher density. The higher dispersion of HNTs in the NR phase could be related to the lower Mooney viscosity of NR in comparison with the EPDM phase. Through the addition of HNTs in the NR phase, the viscosity ratio of the binary blend could approach unity owing to the rise in the viscosity of NR phase.⁶¹ As the viscosity ratio approaches unity, the minor phase, that is, EPDM here, reaches a minimal size domain⁶² due to the improved interface between the two phases evidenced by FE-SEM images.

As reported in the literature, HNTs can be uniformly and readily dispersed in elastomer matrices as compared to other natural silicate counterparts such as montmorillonite and kaolinite.⁶³⁻⁶⁴ This is as a result of the specific array of HNT lumens, including straight tube-like morphology, anomalous charge distribution, low hydroxyl density on the surfaces, and unique crystal structure. Even though the dispersion morphology of both the 8 phr and 10 phr based nanocomposites was more or less equal, there was some minor agglomeration formation of the HNTs in the 10 phr formulation (Figure 11(c)), which can be indicative of stronger interaction between HNTs as compared to the interaction between HNT and elastomer matrix.⁶⁵

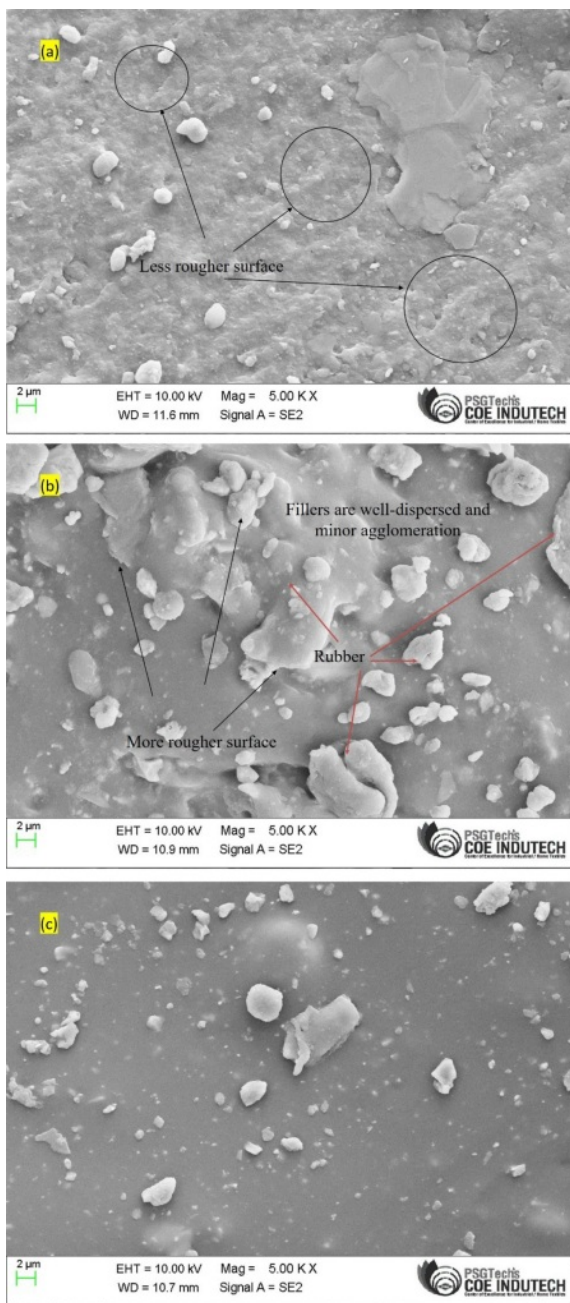


Figure 11. The tensile fractured surfaces with magnification $X = 1000$ of nanotubes filled EPDM/NBR composites: (a) H_0 ; (b) H_8 ; (c) H_{10} .

Conclusions

In this study, HNTs were employed to improve the overall performance of NR/EPDM/EPDM-*g*-MA/HNTs nanocomposites for engineering applications. To this end, the effect of HNTs loading on the cure characteristics, mechanical, physical, and swelling properties of NR/EPDM/EPDM-*g*-MA/HNTs nano-

composites was investigated in detail. HNTs-reinforced rubber samples displayed a slower crosslink rate with more rough fracture surface indicating an effective interaction between the elastomer chains and HNTs and fine dispersion of HNTs, particularly below 8 phr of HNTs that was confirmed by FE-SEM. The incorporated HNTs were able to provide superior protection of the NR/EPDM/EPDM-*g*-MA/HNTs nanocomposites against solvents exposure owing to the penetration hindrance provided by the fine dispersion of the HNTs and improved rubber/HNT interactions. The tensile strength, hardness and abrasion resistance of NR/EPDM were also substantially enhanced by the HNTs incorporation at the cost of a slight but significant reduction in the rebound resilience. The considerable improvement in the cure torques, curing times, swelling behavior, abrasion resistance, tensile strength, hardness and tear strength of NR/EPDM nanocomposites indicated that the incorporation of appropriate levels of HNT nanofillers in NR/EPDM and other similar elastomers is a very appealing platform to transform such elastomers into good performance materials for a range of engineering applications used in demanding environments.

References

1. Bhowmick, A. K.; Chakraborty, B. Bond Strength in Various Rubber-to-rubber Joints. *Plast. Rubber Process. Appl.* **1989**, *11*, 99-106.
2. Vishvanathperumal, S.; Navaneethakrishnan, V.; Anand, G.; Gopalakannan, S. Evaluation of Crosslink Density Using Material Constants of Ethylene-propylene-Diene Monomer/styrene-butadiene Rubber with Different Nanoclay Loading: Finite Element Analysis-simulation and Experimental. *Adv. Sci. Eng. Medicine* **2020**, *12*, 632-642.
3. Theja, R.; Kilari, N.; Vishvanathperumal, S.; Navaneethakrishnan, V. Modeling Tensile Modulus of Nanoclay-filled Ethylene-propylene-diene Monomer/styrene-butadiene Rubber Using Composite Theories. *J. Rubber Res.* **2021**, *24*, 847-856.
4. Costa, V. G.; Nunes, R. C. R. Mechanical Properties of Blends of EPDM with NR-cellulose II System. *Eur. Polym. J.* **1994**, *30*, 1025-1028.
5. Cheremisinoff, N. P. Spotlight on EPDM Elastomers. *Polym. Plast. Technol. Eng.* **1992**, *31*, 713-744.
6. Coran, A. Y. Anisotropy of Ultimate Properties in Vulcanizates of EPDM/high-diene-rubber Blends. *Rubber Chem. Technol.* **1991**, *64*, 801-812.
7. Shehata, A. B.; Afifi, H.; Darwish, N. A.; Mounir, A. Evaluation of the Effect of Polymeric Compounds as Compatibilizers for NR/EPDM Blend. *Polym. Plast. Technol. Eng.* **2006**, *45*, 165-170.
8. Xiao, X.; Chevali, V. S.; Song, P.; Yu, B.; Yang, Y.; Wang, H. Enhanced Toughness of PLLA/PCL Blends Using Poly(*d*-lactide)-Poly(ϵ -caprolactone)-poly(*d*-lactide) as Compatibilizer. *Compos.*

- Commun.* **2020**, *21*, 100385.
9. Nabil, H.; Ismail, H.; Azura, A. R. Comparison of Thermo-oxidative Ageing and Thermal Analysis of Carbon Black-filled NR/Virgin EPDM and NR/Recycled EPDM Blends. *Polym. Test.* **2013**, *32*, 631-639.
 10. Han, T.; Nagarajan, S.; Zhao, H.; Sun, C.; Wen, S.; Zhao, S.; Zhao, S.; Zhang, L. Novel Reinforcement Behavior in Nanofilled Natural Rubber (NR)/butadiene-acrylonitrile Rubber (NBR) Blends: Filling-polymer Network and Supernanosphere. *Polymer* **2020**, *186*, 122005.
 11. Salzano de Luna M.; Filippone, G. Effects of Nanoparticles on the Morphology of Immiscible Polymer Blends Challenges and Opportunities. *Eur. Polym. J.* **2016**, *79*, 198-218.
 12. Krause, IC. Polymer-polymer Compatibility. In: Paul DR, Bucknall CB (eds) *Polymer Blends*. John Wiley & Sons, Inc, New York, 2000, 15-30.
 13. Ibarra, L.; Rodríguez, A.; Mora, I. Ionic Nanocomposites Based on XNBR-OMg Filled with Layered Nanoclays. *Eur. Polym. J.* **2007**, *43*, 753-761
 14. Sae-oui, P.; Sirisinha, C.; Thepsuwan, U.; Thapthong, P. Influence of Accelerator Type on Properties of NR/EPDM Blends. *Polym. Test.* **2007**, *26*, 1062-1067.
 15. Botros, S. H.; Tawfic, M. L. Synthesis and Characteristics of MAH-g-EPDM Compatibilized EPDM/NBR Rubber Blends. *J. Elastomers Plast.* **2006**, *38*, 349-365.
 16. Zhang, H.; Datta, R. N.; Talma, A. G.; Noordermeer, J. W. Maleic-anhydride Grafted EPM as Compatibilising Agent in NR/BR/EPDM Blends. *Eur. Polym. J.* **2010**, *46*, 754-766.
 17. Zaharescu, T.; Meltzer, V.; Vilcu, R. Thermal Properties of EPDM/NR Blends. *Polym. Degrad. Stab.* **2000**, *70*, 341-345.
 18. Ananchaenwong, E.; Marthosa, S.; Suklueng, M.; Niyomwas, S.; Chaiprapat, S. Effect of Silicon Carbide on the Properties of Natural Rubber Blends with EPDM Rubber. *Int. J. Integrated Eng.* **2020**, *12*, 234-240.
 19. Vishvanathperumal, S.; Gopalakannan, S. Effects of the Nanoclay and Crosslinking Systems on the Mechanical Properties of Ethylene-propylene-diene Monomer/styrene Butadiene Rubber Blends Nanocomposite. *Silicon* **2019**, *11*, 117-135.
 20. Vishvanathperumal, S.; Anand, G. Effect of Nanoclay/nanosilica on the Mechanical Properties, Abrasion and Swelling Resistance of EPDM/SBR Composites. *Silicon* **2020**, *12*, 1925-1941.
 21. Vishvanathperumal, S.; Anand, G. Effect of Nanosilica and Crosslinking System on the Mechanical Properties and Swelling Resistance of EPDM/SBR Nanocomposites with and Without TESPT. *Silicon* **2021**, *13*, 3473-3497.
 22. Vishvanathperumal, S.; Anand, G. Effect of Nanosilica on the Mechanical Properties, Compression Set, Morphology, Abrasion and Swelling Resistance of Sulphur Cured EPDM/SBR Composites. *Silicon* **2022**, *14*, 3523-3534.
 23. Vishvanathperumal, S.; Gopalakannan, S. Reinforcement of Ethylene Vinyl Acetate with Carbon Black/silica Hybrid Filler Composites. *Appl. Mech. Mater.* **2016**, *852*, 16-22.
 24. Thomas, S.; Stephen, R. *Rubber Nanocomposites: Preparation, Properties and Applications*; John Wiley and Sons: Singapore, 2010.
 25. Vishvanathperumal, S.; Navaneethakrishnan, V.; Gopalakannan, S. The Effect of Nanoclay and Hybrid Filler on Curing Characteristics, Mechanical Properties and Swelling Resistance of Ethylene-vinyl Acetate/styrene Butadiene Rubber Blend Composite. *J. Adv. Microscopy Res.* **2018**, *13*, 469-476.
 26. Rezende, C. A.; Bragança, F. C.; Doi, T. R.; Lee, L. T.; Galembeck, F.; Boué, F. Natural Rubber-clay Nanocomposites: Mechanical and Structural Properties. *Polymer* **2010**, *51*, 3644-3652.
 27. Yu, Y.; Gu, Z.; Song, G.; Li, P.; Li, H.; Liu, W. Structure and Properties of Organo-montmorillonite/nitrile Butadiene Rubber Nanocomposites Prepared From Latex Dispersions. *Appl. Clay Sci.* **2011**, *52*, 381-385.
 28. Hernández, M.; del Mar Bernal, M.; Verdejo, R.; Ezquerro, T. A.; López-Manchado, M. A. Overall Performance of Natural Rubber/graphene Nanocomposites. *Compos. Sci. Technol.* **2012**, *73*, 40-46.
 29. Potts, J. R.; Shankar, O.; Murali, S.; Du, L.; Ruoff, R. S. Latex and Two-roll Mill Processing of Thermally-exfoliated Graphite Oxide/natural Rubber Nanocomposites. *Compos. Sci. Technol.* **2013**, *74*, 166-172.
 30. Bauhofer, W.; Kovacs, J. Z. A Review and Analysis of Electrical Percolation in Carbon Nanotube Polymer Composites. *Compos. Sci. Technol.* **2009**, *69*, 1486-1498.
 31. Lvov, Y. M.; Shchukin, D. G.; Mohwald, H.; Price, R. R. Halloysite Clay Nanotubes for Controlled Release of Protective Agents. *ACS Nano*, **2008**, *2*, 814-820.
 32. Shchukin, D. G.; Lamaka, S. V.; Yasakau, K. A.; Zheludkevich, M. L.; Ferreira, M. G. S.; Möhwald, H. Active Anticorrosion Coatings with Halloysite Nanocontainers. *J. Phys. Chem. C*, **2008**, *112*, 958-964.
 33. Guimaraes, L.; Enyashin, A. N.; Seifert, G.; Duarte, H. A. Structural, Electronic, and Mechanical Properties of Single-walled Halloysite Nanotube Models. *J. Phys. Chem. C*, **2010**, *114*, 11358-11363.
 34. Vergaro, V.; Abdullayev, E.; Lvov, Y. M.; Zeitoun, A.; Cingolani, R.; Rinaldi, R.; Leporatti, S. Cytocompatibility and Uptake of Halloysite Clay Nanotubes. *Biomacromolecules* **2010**, *11*, 820-826.
 35. Alipour, A.; Naderi, G.; Bakhshandeh, G. R.; Vali, H.; Shokoohi, S. Elastomer Nanocomposites Based on NR/EPDM/Organoclay: Morphology and Properties. *Int. Polym. Proc.* **2011**, *26*, 48-55.
 36. Anand, G.; Vishvanathperumal, S. Properties of SBR/NR Blend: The Effects of Carbon Black/Silica (CB/SiO₂) Hybrid Filler and Silane Coupling Agent. *Silicon* **2022**, *14*, 9051-9060.
 37. Vishvanathperumal, S.; Gopalakannan, S. Swelling Properties, Compression Set Behavior and Abrasion Resistance of Ethylene-propylene-diene Rubber/styrene Butadiene Rubber Blend Nanocomposites. *Polym. Korea* **2017**, *41*, 433-442.
 38. Senthilvel, K.; Vishvanathperumal, S.; Prabu, B.; John Baruch, L. Studies on the Morphology, Cure Characteristics and Mechanical Properties of Acrylonitrile Butadiene Rubber with Hybrid Filler (carbon black/silica) Composite. *Polym. Polym. Compos.* **2016**, *24*, 473-480.
 39. Manoj, K. C.; Kumari, P.; Rajesh, C.; Unnikrishnan, G. Aromatic

- Liquid Transport Through Filled EPDM/NBR Blends. *J. Polym. Res.* **2010**, *17*, 1-9.
40. Flory, P. J.; Rehner, J. Statistical Mechanics of Cross-Linked Polymer Networks I. Rubberlike Elasticity. *J. Chem. Phys.* **1943**, *11*, 512.
 41. Sujith, A.; Unnikrishnan, G. Molecular Sorption by Heterogeneous Natural Rubber/poly(ethylene-co-vinyl acetate) Blend Systems. *J. Polym. Res.* **2006**, *13*, 171-180.
 42. Thomas, P. C.; Tomlal Jose E.; Selvin Thomas, P.; Thomas, S.; Joseph, K. High-performance Nanocomposites Based on Acrylonitrile-butadiene Rubber with Fillers of Different Particle Size: Mechanical and Morphological Studies. *Polym. Compos.* **2010**, *31*, 1515-1524.
 43. M. O. Abou-Helal, S. H. El-Sabbagh, A Study on the Compatibility of NR-EPDM Blends Using Electrical and Mechanical Techniques, *J. Elastomers Plast.* **2005**, *37*, 319-346.
 44. Noriman, N. Z.; Ismail, H. Properties of Styrene Butadiene Rubber (SBR)/recycled Acrylonitrile Butadiene Rubber (NBRr) Blends: the Effects of Carbon Black/silica (CB/silica) Hybrid Filler and Silane Coupling Agent, Si69. *J. Appl. Polym. Sci.* **2012**, *124*, 19-27.
 45. Ismail, H.; Rosnah, N.; Rozman, H. Curing Characteristics and Mechanical Properties of Short Oil Palm Fibre Reinforced Rubber Composites. *Polymer* **1997**, *38*, 4059-4064.
 46. Ismail, H.; Anuar, H. Palm Oil Fatty Acid as An Activator in Carbon Black Filled Natural Rubber Compounds: Dynamic Properties, Curing Characteristics, Reversion and Fatigue Studies. *Polym. Test.* **2000**, *19*, 349-359.
 47. Ismail, H.; Freakley, P. K.; Sutherland, I.; Sheng, E. Effects of Multifunctional Additive on Mechanical Properties of Silica Filled Natural Rubber Compound. *Eur. Polym. J.* **1995**, *31*, 1109-1117.
 48. Paran, S. M. R.; Naderi, G.; Javadi, F.; Shemshadi, R.; Saeb, M. R. Experimental and Theoretical Analyses on Mechanical Properties and Stiffness of Hybrid Graphene/graphene Oxide Reinforced EPDM/NBR Nanocomposites. *Mater. Today Commun.* **2020**, *22*, 100763.
 49. Ismail, H.; Salleh, S. Z.; Ahmad, Z. Properties of Halloysite Nanotube (HNT) Filled SMR L and ENR 50 Nanocomposites. *Int. J. Polym. Mater. Polym. Biomater.* **2013**, *62*, 314-322.
 50. Pasbakhsh, P.; Ismail, H.; Fauzi, M. A.; Bakar, A. A. Influence of Maleic Anhydride Grafted Ethylene Propylene Diene Monomer (MAH-g-EPDM) on the Properties of EPDM Nanocomposites Reinforced by Halloysite Nanotubes. *Polym. Test.* **2009**, *28*, 548-559.
 51. Ganeche, P. S.; Balasubramanian, P.; Vishvanathperumal, S. Halloysite Nanotubes (HNTs)-Filled Ethylene-Propylene-Diene Monomer/Styrene-Butadiene Rubber (EPDM/SBR) Composites: Mechanical, Swelling, and Morphological Properties. *Silicon* **2022**, *14*, 6611-6620.
 52. Sundar, R.; Mohan, S. K.; Vishvanathperumal, S. Effect of Surface Modified Halloysite Nanotubes (mHNTs) on the Mechanical Properties and Swelling Resistance of EPDM/NBR Nanocomposites. *Polym. Korea* **2022**, *46*, 728-743.
 53. Zhixin, J.; Yuanfang, L.; Shuyan, Y.; Mingliang, D.; Baochun, G.; Demin, J. Styrene-butadiene Rubber/halloysite Nanotubes Composites Modified by Epoxidized Natural Rubber. *J. Nanosci. Nanotechnol.* **2011**, *11*, 10958-10962.
 54. Alipour, A.; Naderi, G.; Ghoreishy, M. H. Effect of Nanoclay Content and Matrix Composition on Properties and Stress-strain Behavior of NR/EPDM Nanocomposites. *J. Appl. Polym. Sci.* **2013**, *127*, 1275-1284.
 55. Pasbakhsh, P.; Ismail, H.; Fauzi, M. A.; Bakar, A. A. Influence of Maleic Anhydride Grafted Ethylene Propylene Diene Monomer (MAH-g-EPDM) on the Properties of EPDM Nanocomposites Reinforced by Halloysite Nanotubes. *Polym. Test.* **2009**, *28*, 548-559.
 56. Ramesh, P.; Joseph, R.; Sunny, M. C. A Comparative Evaluation of Coefficient of Friction and Mechanical Properties of Commercially Available Foley Catheters. *J. Biomater. Appl.* **2001**, *15*, 344-350.
 57. Maiti, M.; Bhowmick, A. K. Effect of Polymer-clay Interaction on Solvent Transport Behavior of Fluoroelastomer-clay Nanocomposites and Prediction of Aspect Ratio of Nanoclay. *J. Appl. Polym. Sci.* **2007**, *105*, 435-445.
 58. Stephen, R.; Varghese, S.; Joseph, K.; Oommen, Z.; Thomas, S. Diffusion and Transport Through Nanocomposites of Natural Rubber (NR) Carboxylated Styrene Butadiene Rubber (XSBR) and Their Blends. *J. Memb. Sci.* **2006**, *282*, 162-170.
 59. Movahed, S. O.; Ansarifard, A.; Mirzaie, F. Effect of Various Efficient Vulcanization Cure Systems on the Compression Set of a Nitrile Rubber Filled with Different Fillers. *J. Appl. Polym. Sci.* **2015**, *132*, DOI: 10.1002/APP.41512.
 60. Ragupathy, K.; Prabakaran, G.; Pragadish, N.; Vishvanathperumal, S. Effect of Silica Nanoparticles and Modified Silica Nanoparticles on the Mechanical and Swelling Properties of EPDM/SBR Blend Nanocomposites. *Silicon* **2023**, DOI: 10.1007/S12633-023-02497-1
 61. Ghaderzadeh, S.; Esmizadeh, E.; Vahidifar, A.; Naderi, G.; Ghoreishy, M. H. R.; Mekonnen, T. H. Naturally Occurring Halloysite Nanotubes for Enhanced Durability of Natural Rubber/ethylene Propylene Diene Monomer Rubber Vulcanizate. *J. Vinyl Additive Technol.* **2021**, *27*, 855-867.
 62. Rastin, H.; Jafari, S. H.; Saeb, M. R.; Khonakdar, H. A.; Wagenknecht, U.; Heinrich, G. On the Reliability of Existing Theoretical Models in Anticipating Type of Morphology and Domain Size in HDPE/PA-6/EVOH Ternary Blends. *Europ. Polym. J.* **2014**, *53*, 1-12.
 63. Pasbakhsh, P.; Ismail, H.; Mohd Nor, A. F.; Abu Bakar, A. Electron Beam Irradiation of Sulphur Vulcanised Ethylene Propylene Diene Monomer (EPDM) Nanocomposites Reinforced by Halloysite Nanotubes. *Plastics, Rubber and Compos.* **2012**, *41*, 430-440.
 64. Rooj, S.; Das, A.; Thakur, V.; Mahaling, R. N.; Bhowmick, A. K.; Heinrich, G. Preparation and Properties of Natural Nanocomposites Based on Natural Rubber and Naturally Occurring Halloysite Nanotubes. *Mater. Design* **2010**, *31*, 2151-2156.
 65. Das, R. K.; Ragupathy, K.; Kumar, T. S.; Vishvanathperumal, S. Effect of Halloysite Nanotubes (HNTs) on Mechanical Properties of EPDM/NBR Blend-Nanocomposites. *Polymer Korea* **2023**, *47*, 221-232.

Publisher's Note The Polymer Society of Korea remains neutral with regard to jurisdictional claims in published articles and institutional affiliations.